Transverse Instability of Magnetized Electron Holes

L. Muschietti, I. Roth, C. W. Carlson, and R. E. Ergun*
Space Sciences Laboratory, University of California, Berkeley, California 94720
(Received 24 March 2000)

We study a transverse instability of the nonlinear equilibria known as electron phase-space holes in the presence of a magnetic field. The instability is intrinsically two dimensional and is determined by the dynamics of the trapped electrons. It depends on hole amplitudes, ambient magnetic fields, and the perpendicular velocity spread. The long-standing hole stability problem in multiple dimensions can be characterized by the gyro-to-bounce frequency ratio. A low ratio associated with a small perpendicular velocity spread results in a disintegration of the positive potential spikes.

PACS numbers: 52.35.Sb, 52.35.Qz, 52.65.Rr, 94.20.Rr

Holes in the electron phase space, or phase-space vortices, have been known since early simulations of the two-stream instability [1,2]. They have also been observed in laboratory experiments with a magnetized, plasma-loaded waveguide [3] and have been invoked to interpret bipolar electric pulses measured in the magnetospheric plasma [4–6]. The electron holes are exact, nonlinear solutions to the Vlasov-Poisson equations that involve a clump of electrons trapped in a phase-space vortex. The resulting density inhomogeneity creates a positive potential hump which self-consistently traps the electrons. While they persist for a long time in one-dimensional simulations, e.g. [7], they were seen to disintegrate when allowed to evolve in a space with multiple dimensions [1,8]. 2D simulations with a substantial background magnetic field $\mathbf{B_0}$, however, clearly demonstrated that electron holes can be stable [9–11]. In 2D they form tubes in phase space with the axes directed transverse to $\mathbf{B_0}$. Correspondingly, the associated potentials form positive ridges running transverse to $\mathbf{B_0}$.

This paper addresses the instability of the electron hole due to transverse perturbations and determines how much magnetic field is required to stabilize it. Since the structure is supported by a clump of trapped electrons, parameters characterizing their dynamics can be expected to be essential. Two such parameters are the bounce frequency of the trapped electrons ω_b and their cyclotron frequency Ω_e. As will be shown, the relation between ω_b and Ω_e is the factor determining the stability of the hole structure.

Model.—Let $-e$, m, and $\Omega_e = eB_0/(mc)$ be the charge, mass, and cyclotron frequency of an electron, and let $T_{e\parallel}$ ($T_{e\perp}$) be their parallel (perpendicular) temperature defined as second moments with $v_{e\parallel,\perp} = (T_{e\parallel,\perp}/m)^{1/2}$. The dimensionless units used have time in the inverse of the plasma frequency $\omega_e = \sqrt{4\pi e^2 n/m}$, velocity in $v_{e\parallel}$, distance in Debye length $\lambda_d = v_{e\parallel}/\omega_e$, and potential in $mv_{e\parallel}^2/e$. Ions are assumed infinitely massive and do not participate in the instability.

Using observations of stable potential spikes on magnetized field lines [5], we describe the potential structure in the comoving frame along $\mathbf{B_0}$ as

$$\phi(x,y) = \psi \exp(-0.5x^2/\Delta_\parallel^2)\phi_\perp(y) \equiv \phi_0(x)\phi_\perp(y), \tag{1}$$

where x and $\Delta_\parallel$ are the coordinate and half width parallel to $\mathbf{B_0}$, and $\phi_\perp(y)$ describes a transverse profile whose scale is assumed large compared with the electron gyroradius. The trapped electrons gyrate about the magnetic field while they bounce back and forth in the parallel direction. The trajectory of a typical electron in phase space is composed of two oscillators with the cyclotron frequency Ω_e for the transverse motion and the bounce frequency ω_b for the parallel motion:

$$\omega_b = \sqrt{\psi/\Delta_\parallel^2}. \tag{2}$$

If the potential is homogeneous in the transverse direction, $\phi_\perp \to 1$, there exists an exact, stationary solution. The self-consistent electron distribution can be computed by the Bernstein-Greene-Kruskal method. An example was presented in [11]. It reads

$$F(x, v_x, v_y, v_z) = F_1(w)\exp[-0.5(v_y^2 + v_z^2)/T_{e\perp}], \tag{3}$$

where $w \equiv v_x^2 - 2\phi(x)$ is twice the parallel energy and

$$F_1(w) = \frac{\sqrt{-w}}{\pi\Delta_\parallel^2}\left[1 + 2\ln\left(\frac{\psi}{-2w}\right)\right] + \frac{6 + (\sqrt{2} + \sqrt{-w})(1 - w)\sqrt{-w}}{\pi(\sqrt{2} + \sqrt{-w})(4 - 2w + w^2)} \quad \text{for } -2\psi \le w < 0, \tag{4a}$$

$$F_1(w) = \frac{6\sqrt{2}}{\pi(8 + w^3)} \quad \text{for } w > 0. \tag{4b}$$

The trapped distribution (4a) has a hollowed out shape, the logarithm taking negative values about $w \gtrsim -2\psi$, while the passing distribution (4b) has a flattop shape. The condition $F_1(w) > 0$ forms an existence line in $[\Delta_\parallel, \psi]$ parameter space, which dictates a monotonically increasing

 0031-9007/00/85(1)/94(4)$15.00

relation between amplitude and width. This relation stands in contrast to the inverse relation for a standard soliton, but is supported by magnetospheric observations [5,11].

Transverse instability.—We load the distribution function (3) in a 2D particle-in-cell code, and compare the evolution for two cases: gyrofrequency larger and smaller than the bounce frequency. In both cases the initial potential is characterized by $\psi = 0.8$ and $\Delta_\parallel = 3$; hence, $\omega_b \cong 0.3$. Electrons are loaded along x in a way that reproduces the inhomogeneous function $F(x, v_x, v_y, v_z)$. Along the y direction, the particles are distributed in a random, statistically homogeneous way. Ions form a homogeneous neutralizing background. Although a few runs were performed on a larger grid, results shown here are obtained on 32×32 Debye lengths with typically several million particles, hence, a resolution of $\gtrsim 10^3/\lambda_d^2$.

For a gyro-to-bounce frequency ratio larger than unity, the potential structure maintains well its profile, as was shown in [11]. In sharp contrast, Fig. 1 shows the potential evolution for a gyrofrequency (slightly) smaller than the bounce frequency: $\Omega_e = 0.2$ vs $\omega_b = 0.3$. Three successive snapshots ($t = 0, 100, 130$) are displayed by means of contours, the first accompanied by line plots of ϕ in x. The snapshot $t = 100$ reveals a transverse undulation in the contours. The magnitude rapidly increases afterwards, clearly demonstrating an instability. By $t = 140$, the potential structure has been leveled. We stress that the values of the contours do not change, as the instability develops, but their shapes do, indicating a redistribution of the charge density in the transverse direction y. Furthermore, the redistribution appears to take place near the maximum of the potential ($x \sim 16$) as evidenced at $t = 100$. We take it as an indication that the trapped electrons are involved.

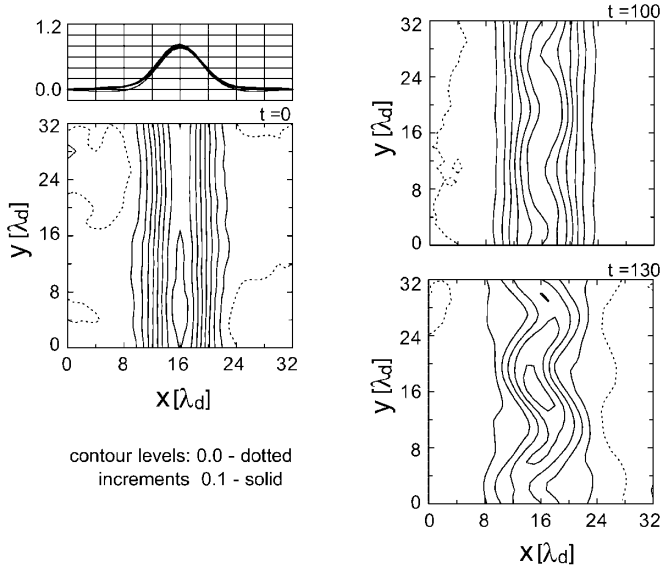

FIG. 1. History of the potential $\phi(x, y)$ where x is parallel to $\mathbf{B_0}$. Unstable case ($\Omega_e = 0.2 < \omega_b = 0.3$). Three snapshots of contours at time = 0, 100, 130. (Upper left) Cuts in x at $y = 8, 16, 24$ of the initial potential. The structure is destroyed by a transverse instability. By $t = 140$ (not shown) the potential hump is leveled. Units: distance λ_d, time ω_e^{-1}, potential $T_{e\parallel}/e$.

Analysis.—The stability analysis of a nonlinear equilibrium such as the one presented here entails assuming an arbitrary perturbation and integrating the Vlasov equation along characteristics defined by the nonlinear particle orbits. The integration provides us with the perturbed distribution function that is then combined with the Poisson equation to yield a dispersion relation [8,12]. The task is rather formidable in the case of the trapped electrons, whose orbits both bounce and gyrate. Instead, we use particle in cell (PIC) simulations and numerically investigate the evolution of the perturbation. Propagation of the information along the trapped orbits will automatically be accounted for.

To this end, we first model the perturbation of the potential observed in runs such as the one presented in Fig. 1, and modify accordingly the equilibrium potential. The combined potential reads

$$\phi(x, y) = \psi \exp\left[-0.5\left(\frac{x - \epsilon \Delta_\parallel \cos ky}{\Delta_\parallel} \right)^2 \right], \quad (5)$$

where $\epsilon < 1$ is a measure of the perturbation and k is its transverse wave number.

To start the simulations, electrons are loaded at time $t = 0$ so as to produce potential (5). The result is shown in Figs. 2(a) and 2(aa) by means of contours in the $[x, y]$ plane for the following parameters: $\psi = 1$, $\Delta_\parallel = 3$,

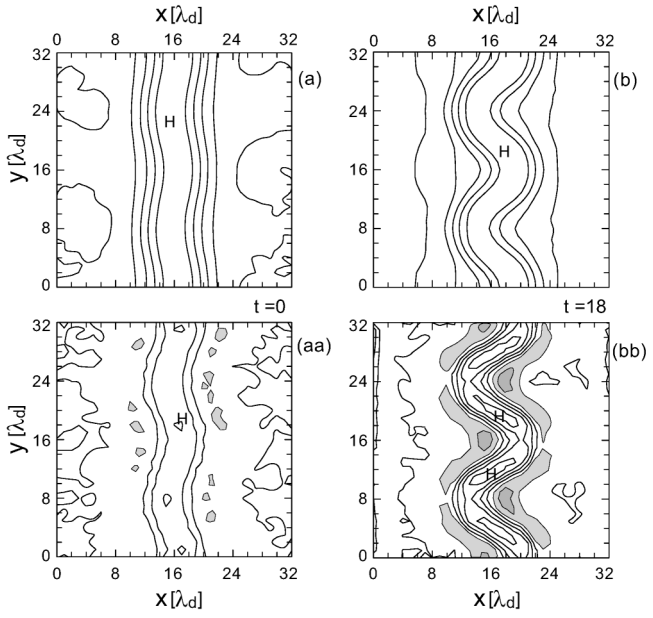

FIG. 2. Initial perturbation and evolution after a bounce period when $\Omega_e < \omega_b$. (a) and (b): Potential $\phi(x, y)$ with contours from 0.0 to 0.8 by increments of 0.2. "H" refers to high. (aa) and (bb): Charge density associated $\rho(x, y)$. Solid contours for $\rho = 0.0, 0.05$, and 0.1; light gray shading for $\rho \lesssim -0.05$; darker gray, $\rho \lesssim -0.1$. Note the electron accumulation and the associated dramatic increase in the undulation of the potential. For details, see text.

$k = 0.39$, and $\epsilon = 0.3$. A translation in x has been performed to center the potential structure around $x = 16$. Panel 2(a) displays $\phi(x, y)$ with contour levels from 0.0 to 0.8 by steps of 0.2. Note the transverse undulation of the contours, especially near the potential high, marked with "H." Panel 2(aa) displays the associated charge density $\rho(x, y)$. We use solid contours at levels 0.0, 0.05, and 0.1, and gray shading to indicate negative $\rho \lesssim -0.05$. As expected, one has a band of positive charge density (the electron hole) surrounded by areas of negative ρ. By differentiating (5), then expanding in ϵ, one can check that the charge density $\rho_0(x) + \epsilon\rho_1(x, y)$ is made of, respectively,

$$\rho_0(x) = \phi_0(x)\,(\Delta_\parallel^2 - x^2)/\Delta_\parallel^4\,, \tag{6}$$

$$\rho_1(x, y) = \phi_0(x)\,(3\Delta_\parallel^2 + k^2\Delta_\parallel^4 - x^2)x\cos(ky)/\Delta_\parallel^5\,. \tag{7}$$

The unperturbed charge density is symmetric in x, while the perturbation is asymmetric in x and has a periodic variation in y, as seen in panel 2(aa).

Several runs were carried out with varying parameters such as Ω_e and $T_{e\perp}$, while keeping $\psi = 1$ and $\Delta_\parallel = 3$; hence, $\omega_b = 0.33$. To illustrate the evolution when the ratio of cyclotron-to-bounce frequency is less than unity (and $v_{e\perp} = 0.1$), Figs. 2(b) and 2(bb) show a snapshot after a bounce period. From the charge density plots, the grey spots are conspicuously growing, which indicates an accumulation of electrons in particular locales. These electron-rich spots are defined by the concave portions of the potential contours, e.g., $x \approx 20$ and $y \approx 8$. As trapped electrons move in the potential well, they are focused by the transverse gradients of the potential into those areas that already have a surplus of electrons, in agreement with (7). This means that the transverse undulation in the potential becomes more pronounced as seen from panel 2(a) to 2(b).

The principle is illustrated in Fig. 3, which depicts electron trajectories in $[x, y]$ of particles that have no perpendicular kinetic energy. Starting from a turning point, equations of motion in the potential given by (5) are integrated for a little over half-a-bounce period. The left and right display shows trajectories initiated at the left and the right turning point, respectively. Because the focusing brings electrons into locales that already have a surplus of electrons, the perturbed potential is enhanced, leading to an instability. The characteristic time scale is expected to be given by the bounce period.

Additional evidence of the focusing can be found by inspecting electron distribution functions (not shown) from the PIC simulation of Fig. 2. The fluxes of trapped electrons about $x \sim 16$ are clearly asymmetric with more particles moving to the right where $y \sim 8$ and conversely where $y \sim 16$.

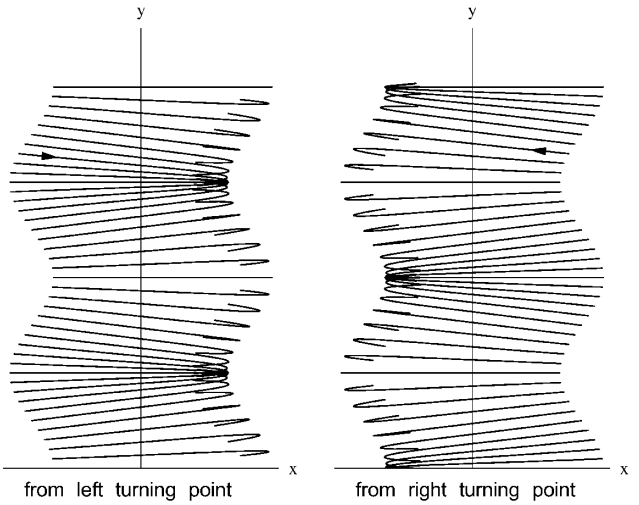

FIG. 3. Trajectories of trapped electrons illustrating the focusing. The display shows the trajectories starting from a turning point for a little over half-a-bounce period. Compare to panel (bb) of Fig. 2.

An effect that can offset the focusing, and thereby prevent the instability, is the spatial dispersion of the electrons during one transit between turning points due to their perpendicular velocity spread $v_{e\perp}$. The focusing requires that $v_{e\perp}$ causes a negligible distortion of the trajectories; i.e., the perturbed perpendicular deviation, for weakly magnetized electrons, needs to be much smaller than the potential wavelength:

$$v_{e\perp} \ll \omega_b/k\,. \tag{8}$$

Increasing $v_{e\perp}$ to 0.2 confirms that less focusing occurs and a run with $v_{e\perp} = 1.0$ shows no instability.

The unstable run presented in Fig. 2 had $\Omega_e < \omega_b$. If one increases the magnetic field such that $\Omega_e > \omega_b$, leaving everything else the same, the y undulation decays after a few oscillations. As the trapped electrons bounce back and forth, the magnetic field guides them and prevents them from being focused by the transverse gradients of the potential. The nonlinear equilibrium is thus stable.

Discussion.—We have studied a transverse instability of the nonlinear equilibria known as electron holes that is due to the motion of the trapped electrons. In this sense it is reminiscent of the sideband instability of a large amplitude wave [12,13]. However, the physics is intrinsically two dimensional and quite different. The transverse gradients of the potential focus the trapped electrons into locales that already have a surplus of electrons, which results in larger transverse gradients and thus more focusing. It is thus a self-focusing type of instability that acts at the level of the particle trajectories. Note that the instability is determined by the dynamics of individual particles and not necessarily by their collective response to a perturbation. To occur, it requires the ratio of gyro-to-bounce frequency to be less than unity and it is favored by anisotropic distribution functions with a narrow spread in the transverse direction.

The present analysis explains the long-known results that simulations of the two-stream instability can lead to long-life electron holes in a one-dimensional geometry but not in geometries with multiple dimensions [1]. Those simulations, having no background magnetic field, automatically satisfy the transverse instability criterion. Furthermore, distribution functions relaxed from an initial two-stream configuration are anisotropic with a comparatively small perpendicular velocity spread.

The theory also applies to more recent simulations that include a background magnetic field $\mathbf{B_0}$. While [9,11] assume a strong magnetic field such that $\Omega_e = 5\omega_e$, [10,14] consider weaker fields. In particular, [14] observed two classes of coherent potential structures appearing in their simulations; while the large structures were quickly unstable, the weaker ones were stable. Applying with hindsight the gyro-to-bounce criterion, the large, unstable structures are found to have a sufficient electric field to satisfy $\omega_b > \Omega_e$ and conversely for the weaker ones [15].

We emphasize that the instability described here is different from another instability recently discussed [16] that was observed in simulations of a strongly magnetized plasma, in which $\Omega_e = 5\ \omega_e > \omega_b$. The instability, which was slow to develop, involving time scales of hundreds of ω_e^{-1}, had no connection to trapping yet involved the emission of electrostatic whistlers.

Recent satellite measurements of bipolar electric spikes have been interpreted as signatures of phase-space holes. Three spacecraft, FAST, Polar, and Geotail, all equipped with a wave form capture receiver, yet following very different orbits, have gathered data on electron holes in various parts of the magnetosphere. (See, e.g., [4] for Geotail, [6] for Polar, and [5] for FAST.) Our results are consistent with the global trend of the data. The most intense electric fields are observed close to Earth where the magnetic field is the strongest, meaning a higher cyclotron frequency. This allows for a faster bounce ω_b and thus larger electric fields. Finally, since the nonlinear potential spikes have been associated with parallel electric fields [5], their stability is crucial for anomalous resistivity and, hence, the formation of electric fields in many magnetized, astrophysical objects.

The simulations were performed using the Cray T90 of San Diego Supercomputer Center. The research was supported by the following grants from NASA: NAG5-6985, NAG5-4898, NAG5-3596, and NAG5-3182.

*Present address: LASP, University of Colorado, Boulder, CO 80303.

[1] R. L. Morse and C. W. Nielson, Phys. Rev. Lett. **23**, 1087 (1969).
[2] H. L. Berk, C. E. Nielsen, and K. V. Roberts, Phys. Fluids **13**, 980 (1970).
[3] J. P. Lynov *et al.*, Phys. Scr. **20**, 328 (1979).
[4] H. Matsumoto *et al.*, Geophys. Res. Lett. **21**, 2915 (1994).
[5] R. E. Ergun *et al.*, Phys. Rev. Lett. **81**, 826 (1998).
[6] J. R. Franz, P. M. Kintner, and J. S. Pickett, Geophys. Res. Lett. **25**, 1277 (1998).
[7] Y. Omura, H. Matsumoto, T. Miyake, and H. Kojima, J. Geophys. Res. **101**, 2685 (1996).
[8] H. Schamel, Phys. Rev. Lett. **48**, 481 (1982).
[9] M. V. Goldman, M. M. Oppenheim, and D. L. Newman, Geophys. Res. Lett. **26**, 1821 (1999).
[10] T. Miyake, Y. Omura, H. Matsumoto, and H. Kojima, J. Geophys. Res. **103**, 11 841 (1998).
[11] L. Muschietti, I. Roth, R. E. Ergun, and C. W. Carlson, Nonlinear Proc. Geophys. **6**, 211 (1999); Geophys. Res. Lett. **26**, 1093 (1999); Geophys. Res. Lett. **26**, 1689 (1999).
[12] M. V. Goldman, Phys. Fluids **13**, 1281 (1970).
[13] W. L. Kruer and J. M. Dawson, Phys. Fluids **13**, 2747 (1970).
[14] F. Mottez, S. Perraut, and A. Roux, J. Geophys. Res. **102**, 11 399 (1997).
[15] F. Mottez (private communication).
[16] M. Oppenheim, D. L. Newman, and M. V. Goldman, Phys. Rev. Lett. **83**, 2344 (1999).